PCCP

Accepted Manuscript

ROYAL SOCIETY OF CHEMISTRY

www.rsc.org/pccp

Comparative theoretical study of metal functionalized carbon nanocone and carbon nanocone sheet as potential hydrogen storage materials

A.S.Shalabi[1*], K.A.Soliman[1], H.O.Taha[2]

[1] Department of Chemistry, Faculty of Science, Benha University,
P.O.Box 13518, Benha, Egypt.
[2] Department of Physics, Faculty of Education, Ain Shams University,
Roxy, Cairo, Egypt.

Abstract

The hydrogen storage of Ti functionalized carbon nanocone and carbon nanocone sheet is investigated by using the state of the art density functional theory calculations. The Ti atom prefers to bind at the hollow site of the hexagonal ring. The average adsorption energies corrected for dispersion forces are -0.54 and -0.39 eV per hydrogen molecule. With no metal clustering, the system gravimetric capacities are expected to be as large as 9.31 and 11.01 wt%. The hydrogen storage reactions are characterized in terms of simulated infrared spectra, projected densities of states, kinetics, and statistical thermodynamics. The free energies and enthalpies of the Ti functionalized carbon nanocone meet the ultimate targets of the department of energy for all temperatures and pressures. The closest reactions to zero free energy occur at (378.15 K/2.961 atm.) for carbon nanocone and (233.15 K/2.961 atm.) for carbon nanocone sheet. The translational component is found to exact a dominant effect on the total entropy change with temperature. More promising thermodynamics are assigned to the hydrogenation of Ti functionalized carbon nanocone sheet at 233.15 K. As the temperature is increased, the life times of the hydrogen molecules adsorbed at the surface drop and the rate constants increase. At fixed pressure, the rate constants of hydrogentation of Ti functionalized carbon nanocone are smaller than those of Ti functionalized carbon nanocone sheet, while the life times are greater.

Key words: comparative study-nanocones-hydrogen storage-dispersion forces-DFT.

[*] Corresponding author: Tel./Fax. : +20-2-24188738/Mob. : +20-100-5211681/
e-mail: asshalabi@hotmail.com (A.S.Shalabi).

Introduction

Hydrogen is a convenient, safe, and versatile fuel source that can be easily converted to a desired form of energy without releasing harmful emissions **[1]**. As an energy carrier used for vehicle applications, hydrogen has several advantages. It has a high energy density by weight, can be produced renewably, and when combined with oxygen in a proton exchange membrane, it can be used to generate power with only water as a by-product **[2]**.

As far as theoretical calculations are concerned, theoretical approaches have proven convenient and supportive in validating and better directing the development of hydrogen storage media. An approach to hydrogen storage utilizes carbon based materials doped with transition metals. Carbon based materials include carbon nanotubes and graphenes. The results for hydrogen storage in carbon nanotubes have led to the emergence of carbon nanocones (CNCs). Single walled CNC consists of single walled graphitic structure formed out of a single graphene sheet rolled up to form conical shape that aggregate to form globular rosette structures with sizes of about 80-100 nm. CNCs exhibit very large surface areas approaching 1500 m^2/g. Because of low cost, high purity and high surface area CNCs became attractive candidates for hydrogen storage. Heats of adsorption corresponding to 100-120 meV have been reported and attributed to enhanced interaction of H_2 molecules at the conical tip of the nanocone **[3]** and in view of their pure (>95%) composition, they have been deemed as ideal models to study hydrogen storage via physisorption **[4]**. At the other hand, a graphene is a single layer of graphite in a hexagonal structure, or an individual sheet of sp^2 hybridized carbon bound in two dimensions **[5]**. A graphene is not an allotrope of carbon, and it was predicted that a single ethylene molecule can form a stable complex with two transition metals, thus absorbing ten H_2 molecules and lead to a high storage capacity of ~14 wt% **[6]**. The advantages of graphenes as potential hydrogen storage materials are: (i) a large surface for hydrogen adsorption (ii) economical and scalable production (iii) the strongest material ever measured **[7]**. However, hydrogen storage of a CNC in comparison with its parent carbon nanocone sheet (CNCS) has not been explored.

The present study explores a comparison between a CNC and its parent CNCS as potential hydrogen storage materials with reference to the ultimate targets of DOE for physisorption, system gravimetric capacity, and thermodynamic properties. The thermodynamics of a hydrogen storage reaction is one of the most fundamental properties of a potential hydrogen storage material. We have therefore draw attention to the thermodynamic capabilities of CNC and CNCS as potential hydrogen storage materials, in addition to some of the kinetic aspects of the relevant reactions.

Computational details

In density functional theory (DFT) the ground state of an interacting electron gas is mapped onto the ground state of a non interacting electron gas. This mapping in principle gives exact ground state properties **[7]**. The advantages of employing DFT calculations for hydrogen storage materials research may be summarized as the accuracy of computed thermodynamic quantities, the efficiency relative to experiment, and thermodynamic predictions of new functionalized nanostructures **[2]**.

Since under regular conditions the hydrogen molecule is a very weakly interacting species, correcting for dispersion interactions is an important requirement. The long-range corrected hybrid density functional with damped atom-atom dispersion corrections wb97xd **[8]** was employed in the calculations. Full geometry optimizations without symmetry constraints were carried out for H_2, CNC, CNCS, Ti-CNC, Ti-CNCS, $4H_2$-Ti-CNC, and $4H_2$-Ti-CNCS at the wb97xd level of theory by using the 6-31G(d,p) basis set. This basis set uses Gaussian type functions (GTOs), adds d-type polarization functions to carbon, f-type polarization functions to titanium, and p-type polarization functions to hydrogen. The thresholds of geometry optimizations are: Maximum Force: 0.002500, RMS Force: 0.001667, Maximum Displacements: 0.010000, and RMS displacements: 0.006667. The convergence criteria of single point SCF energy calculations are: RMS density matrix=1.00D-07, MAX density matrix=1.00D-05, and energy=1.00D-05.

All calculations were carried out by using Gaussian 09 system **[9]**. The projected densities of states (PDOS), and Fermi levels were calculated by using Gauss Sum 2.2.5 which is a post processing of Gaussian 09 code **[10]**. The optimal geometries were visualized by using the corresponding Gauss View 5.0 software.

Results and discussion

We constructed a CNC with disclination angle 180^{o} and height 9 Å, consisting of 69 carbon atoms, and 27 hexagonal rings. The corresponding CNCS consists of 24 hexagonal rings. The optimized geometries of CNC, CNCS, Ti-CNC, Ti-CNCS, 4H_2-Ti-CNC, and 4H_2-Ti-CNCS are shown in **Fig.1**, and the corresponding structural and energetic properties of the optimized systems are given in **Table 1**.

The Ti atom adsorption energies of Ti-CNC and Ti-CNCS are defined as

$$\Delta E_{ads.}(Ti) = E(Ti\text{-}CNC) - E(Ti) - E(CNC) \qquad (1)$$

$$\Delta E_{ads.}(Ti) = E(Ti\text{-}CNCS) - E(Ti) - E(CNCS) \qquad (2)$$

where E(Ti-CNC) and E(Ti-CNCS) are the total energies of the fully relaxed Ti atom deposited on CNC and CNCS, E(Ti) is the energy of the free Ti atom, and E(CNC) and E(CNCS) are the fully relaxed energies of CNC and CNCS. The average adsorption energy of H_2 molecule over Ti -CNC and Ti-CNCS are defined as

$$\Delta E_{ads}(H_2) = [\, E(4H_2\text{-}Ti\text{-}CNC) - 4E(H_2) - E(Ti\text{-}CNC) \,]/n \qquad (3)$$

$$\Delta E_{ads}(H_2) = [\, E(4H_2\text{-}Ti\text{-}CNCS) - 4E(H_2) - E(Ti\text{-}CNCS) \,]/n \qquad (4)$$

where E(4H_2-Ti-CNC) and E(4H_2-Ti-CNCS) are the total energies of the fully relaxed 4H_2-Ti fragments deposited on CNC and CNCS, E(H_2) is the energy of an isolated relaxed hydrogen molecule, E(Ti-CNC) and E(Ti-CNCS) are the total energies of the fully relaxed Ti atom deposited on CNC and CNCS, and (n) is the number of hydrogen molecules. According to the precedent definitions, a negative value of $\Delta E_{ads}(H_2)$ corresponds to an exothermic adsorption.

The distances between Ti and CNCS are shorter than those between Ti and CNC implying stronger binding of Ti to CNCS. The adsorption energies of Ti atom deposited on CNC and CNCS (-3.92 and -5.89 eV) are significantly greater than the average adsorption energies per H_2 (-0.54 and -0.39 eV) ensuring the stability of Ti-CNC and CNCS complexes in the event of H_2 molecule release. The Ti atom prefers to bind at the hollow site of the hexagonal ring, but slightly shifted toward one of the tip carbons. The H_2

internuclear distances are more or less the same in the two complexes, but with elongated bond lengths relative to the experimental bond length of 0.74 Å. The average adsorption energies per H_2 molecule corrected for dispersion forces (-0.54 and -0.39 eV) meet the DOE target for physisorption (-0.20 to -0.60 eV) and nominate both of the CNC and its parent CNCS as potential hydrogen storage materials. Moreover, when the adsorption energies of Ti atom deposited on CNC and CNCS (-3.92 and -5.89 eV) are compared with Ti dimerization energy (-3.88 eV) we come to the conclusion that metal clustering on the upper and lower surfaces of the CNCS is much less probable than that on the outer surface of the CNC. Consequently, if no metal clustering occurs, the hydrogen storage capacities are expected to be as large as 9.31 wt% H_2 on the outer surface of the CNC (with 27 hexagonal rings) and 11.01 wt% H_2 on the upper and lower surfaces of the CNCS (with 48 hexagonal rings). As shown, the two values exceed the ultimate DOE target for system gravimetric capacity of 7.5 wt% H_2.

To shed light on the effect of CNC relative to its parent flat CNCS we consider the out of plane deformation of flat graphene. Investigations of the curvature effects of graphitic nanostructures **[11]** lead to the conclusion that the binding energy of hydrogen on the external surface of nanotubes and fullerenes is increased considerably compared to the flat graphene by values of the order of 1-2 eV depending on the tube diameter and length, on the chirality, on the coverage and type of decoration. As sown in **Table 1**, the average adsorption energy per H_2 molecule on CNC with disclination angle 180 deg. and height 9 Å (-0.59 eV) is considerably greater than that on the flat CNCS (-0.39 eV). The empirical explanation of this effect is that convex surfaces have the sp^2 system distorted towards sp^3 which makes the protruding π orbitals more reactive and prone to bind H **[12]**. To compare our results with CNT decorated with Ti atoms, Yildirim and Ciraci **[13]** reported a first principles study, which demonstrated that a single Ti atom coated on a single walled carbon nanotube (SWCNT) binds up to four hydrogen molecules. They constructed energy vs reaction paths for successive dissociative and molecular adsorption of H_2 over a single Ti coated (8,0) nanotube, and found that the first H_2 adsorption was dissociative with no energy barrier, while the other three adsorptions were molecular. Among the many different isomers they tried for the $4H_2$ system, they found a very symmetric configuration (t80Ti-$4H_2$) with average H-H bond distance (0.84 Å) and average binding energy per H_2 molecule (0.54 eV). These results may be compared with our results of the global minimum fully optimized structure $4H_2$-Ti-CNC with average H-H bond distance (0.79 Å) and average binding energy per H_2 molecule (-0.54 eV).

The positive charges on Ti atoms and the negative charges on the nearest C atoms obtained from natural bond order (NBO) analysis ensure charge transfer from Ti to the CNC and CNCS. Since the hydrogen atoms of the adsorbed H_2 molecule have positive charges, the H_2 molecule cannot be considered as trapped by Ti cation via charge polarization mechanism. This indicates that Ti donates electrons to the neighboring C atoms where the *d*-orbitals of Ti atom overlap with the sp^2 orbitals of Ti-C. This charge transfer behavior leads to Ti atom in cationic form and renders extensive hetero polar bonding between the Ti atom and the nearest neighbor C atoms, resulting in an increase in the H_2 molecule uptake.

The nature of Ti-H bonding can be explained from the analysis of projected densities of states (PDOS) plots. PDOS for *s*- orbital of H and *d*- orbitals of Ti are shown in **Fig.2** . For $4H_2$-Ti- CNC and $4H_2$-Ti- CNCS complexes, the bands of PDOS in the vicinity of the Fermi level highlights that the overlap of Ti-*d* orbitals with H_2-σ* antibonding orbitals is responsible for the formation of Ti-H bond, where the binding state has a major contribution from Ti *d*- orbitals. In the energy range from -15 to -19 eV for $4H_2$-Ti- CNC and -16 to -20 for $4H_2$-Ti- CNCS, the *d*- orbitals of Ti are overlapped with the σ orbitals of the hydrogen molecules, resulting in the H-H bond elongation, where the binding state has a major contribution from H_2-σ orbitals. With the help of NBO analysis, **Table 1**, we identify that the hydrogen atoms have positive charges. This means that while there is no charge transfer from the *d*-orbitals of Ti to the H_2-σ^* orbital of H_2 , there is charge transfer from H_2-σ orbitals to the vacant *d*- orbitals of Ti. This behavior is reflected on the intensities of the PDOS bands, where the intensities of PDOS bands in the regions away from Fermi levels are significantly greater than those in the vicinity of Fermi levels. The general features of $4H_2$-Ti-CNC and $4H_2$-Ti-CNCS complexes plots are different, and the present analysis reveals that only orbital overlap between H-*s* orbitals and Ti-*d* orbitals acts on the adsorbed H_2 molecules.

The numerical harmonic vibrational analysis of the simulated infrared (IR) spectrum was carried out to assign the strongest vibrational modes of molecular hydrogen and to distinguish between $4H_2$-Ti-CNC and $4H_2$-Ti-

CNCS complexes. The modes that are mixed with H_2 vibrations were not taken into account and the calculated IR bands, force constants, and dipole strengths are collected in **Table 3**. Inspection of IR frequencies shows that all of the bands undergo changes in positions and intensities following the unrolling of CNC to its parent CNCS. Up shifts of the whole bands associated with increase of force constants are observed for the CNCS. While the dipole strengths of H(71)-H(72), H(73)-H(74), and H(75)-H(76) molecules decrease with increasing force constants in the CNC, the corresponding dipole strengths in the CNCS increase with increasing force constants.

The thermodynamic properties are a fundamental measure of the hydrogen storage properties of a particular surface. The Ti functionalized surfaces of the CNC and CNCS show global minima on the potential energy surfaces, suggesting that they are dynamically stable structures at 0 K. To calibrate the thermodynamic properties of $4H_2$-Ti-CNC and $4H_2$-Ti-CNCS with the ultimate DOE hydrogen storage targets (-40/95-105 ^{o}C) for (min./max.) H_2 delivery temperature, and (0.3/1.2 MPa) for (min./max.) operating pressure, we calculated the corresponding changes of free energies (ΔG), enthalpies (ΔH), thermal energies ($E_{t.}$), heat capacities at constant volume (C_v), total entropies (ΔS), and the components of entropies ($\Delta S_{elec.}$, $\Delta S_{tran.}$, $\Delta S_{rot.}$, and $\Delta S_{vib.}$). Promising thermodynamics include (-/0 kcal mol^{-1}) for (min./max.) free energy changes, (96/145 Jmol^{-1}k^{-1}) for (min./max.) entropy changes, and (20/50 kJmol^{-1}) for enthalpy changes **[2]**. The thermodynamic properties can be calculated from the standard statistical mechanical equations to include the finite-temperature translational, rotational and vibrational energies. For example, the enthalpy (H) can be calculated as follows

$$H = \sum_{T=0} (E_{elec.} + E_{vib.}) + \sum_{T} (E_{vib.} + E_{rot.} + E_{tran.}) + PV \quad (6)$$

where $E_{elec.}$(T=0 K) is the total electronic energy, $E_{vib.}$(T=0 K) is the zero point vibrational energy (ZPVE) which is a linear sum of the fundamental harmonic frequencies, and $E_{vib.}$(T), $E_{rot.}$(T) and $E_{tran.}$(T) are vibrational, rotational, and translational contributions, respectively. The change in the standard Gibbs free energy is given by

$$\Delta G = \Delta H - T\Delta S \qquad (7)$$

where $$\Delta G = \sum_{\text{Products}} G - \sum_{\text{Reactants}} G \qquad (8)$$

$$\Delta H = \sum_{\text{Products}} H - \sum_{\text{Reactants}} H \qquad (9)$$

$$\Delta S = \sum_{\text{Products}} S - \sum_{\text{Reactants}} S \qquad (10)$$

Similarly, the total entropy (S) and entropy change (ΔS) can be calculated from

$$S = S_{\text{elec.}} + S_{\text{vib.}} + S_{\text{rot.}} + S_{\text{tra.}} \qquad (11)$$

$$\Delta S = \Delta S_{\text{elec.}} + \Delta S_{\text{vib.}} + \Delta S_{\text{rot.}} + \Delta S_{\text{tra.}} \qquad (12)$$

where $S_{\text{elec.}}$, $S_{\text{vib.}}$, $S_{\text{rot.}}$, and $S_{\text{tran.}}$ are the electronic, vibrational, rotational, and translational components of the total entropy (S).

The thermodynamics of the reactions $4H_2$+Ti-CNC and $4H_2$+Ti-CNCS at the ultimate DOE hydrogen storage targets for temperatures and pressures are given in **Table 2**. As shown, the free energy changes (ΔG) of the reactions $4H_2$+Ti-CNC are negative indicating that they are spontaneous and meet the ultimate DOE hydrogen storage targets for all temperatures and pressures. However, the free energy changes (ΔG) of the reactions $4H_2$+Ti-CNCS are negative at 233.15 K only indicating that the reactions are spontaneous and meet the ultimate DOE hydrogen storage targets for all pressures at 233.15 K only. The minimal value of free energy -0.79 kcal/mol is assigned to the $4H_2$+Ti-CNC reaction and -4.54 kcal/mol is assigned to the $4H_2$+Ti-CNCS reaction.

It was perceived that the only way to alter the thermodynamics of a hydrogen storage reaction was to change the composition, and hence the identity, of the storage material itself **[2]**. However, a study involving "destabilized" mixtures of hydrides has altered this perception **[14]**. Destabilization refers to the process of lowering the effective enthalpy of a hydrogen desorption reaction, which, when un-modified would exhibit a ΔH which is too large (i.e ΔH>50 kJ/mol H_2), or too "stable," for practical applications. As shown in **Table 2**, unrolling the CNC lowers the enthalpy changes ΔH and destabilizes the hydrogen storage reactions at the surface of the CNCS. The effects of destabilization identify materials having more promising thermodynamics (ΔH=20-50 kJ/mol H_2) from those likely to be thermodynamic "dead ends" having ($\Delta H<0$ or $\Delta H>80$ kJ/mol H_2) **[2]**. The unrolling the CNC to form the parent CNCS therefore ensures more favorable thermodynamics of hydrogen storage reactions at the surfaces of the CNCS at 233.15 K.

Although both of the changes in enthalpy and entropy increase with increasing temperatures, the changes in free energy decrease. This is because entropy increases faster than enthalpy. To investigate which makes the entropy difference increases faster among electronic, translational, rotational, and vibrational components as the temperature increases, the total entropy components were evaluated. As shown in **Table 2**, the translational component is found to exact a dominant effect on the total entropy change with temperature ~10-11 Cal/mol.K, followed by the vibrational component ~9-10 Cal/mol.K, and rotational component ~3-4 Cal/mol.K. The electronic entropy change is zero.

The present thermodynamic data in the framework of surface coverage, may be analyzed by combining Langmuir equation

$$\theta = \frac{bP}{1+bP} \qquad (13)$$

where θ is the surface coverage, b is the absorption coefficient, and P is the pressure, with van't Hoff relation

$$\ln P = \frac{\Delta H}{RT} - \frac{\Delta S}{R} \qquad (14)$$

where R is the universal gas constant and T is the temperature, to give the following expression for surface coverage θ

$$\theta = \frac{P \exp\left(\frac{-\Delta H}{RT} + \frac{\Delta S}{R}\right)}{1 + P \exp\left(\frac{-\Delta H}{RT} + \frac{\Delta S}{R}\right)} \qquad (15)$$

The surface coverage (θ) at the (min./max.) temperatures (T) and (min./max.) pressures (P) which represent the ultimate targets of DOE for temperatures and pressures are collected in **Table 2**. As shown, while increasing temperature decreases the surface coverage of CNC, it has no effect on the parent CNCS.

Arrhenius equation gives the dependence of the rate constant k of a reaction on the absolute temperature T (K), where A is the pre-exponential factor, frequency factor, or attempt frequency of the reaction (10^{-2} Hz) for H_2 **[15]**, E_a is the activation energy (kJ.mol^{-1}/K), and R is the universal gas constant (~8.309×10^{-3} kJ.mol^{-1})

$$k = A\, e^{[-Ea/RT]} \qquad (16)$$

The units of the attempt frequency A are identical to those of the rate constant and will vary depending on the order of reaction. If the reaction is first order it has the units of (s^{-1}). A is the total number of collisions , leading to a reaction or not per second and $e^{[-Ea/RT]}$ is the probability that any given collision will result in a reaction. It turns out that either increasing the temperature or decreasing the activation energy will result in an increase in rate of rate of reaction. The activation energy barrier Ea was calculated from the relation

$$Ea = \Delta H + RT \qquad (17)$$

where ΔH is the enthalpy change, R is the universal gas constant, and T is the absolute temperature. consequently

$$k = A\, e^{[-(\Delta H+RT)/RT]} \qquad (18)$$

At the other hand, when we come to consider the life time of an adsorbate on a particular surface, we note that adsorption and desorption are often reversible processes. For a single first order process, we can express the life time of the adsorbate on the surface (τ) through Frenkel equation

$$\tau = 1/k \qquad (19)$$

It states that the adsorbate life time on the surface is finite, and that it depends on the temperature and desorption activation energy. As the temperature increases, the life time drops, but even at high temperature there is a finite life time.

The life times τ (s) and rate constants k (s^{-1}) of the reactions $4H_2$+Ti-CNC and $4H_2$+Ti-CNCS at (min.T/min.P) and (max.T/min.P) are collected in **Table 4**. As shown, increasing the temperature (at fixed pressure) drops the life times τ (s) and increases the rate constants k (s^{-1}) of both reactions. This implies more favorable kinetics of the two reactions at the temperatures targeted by DOE, regardless of the applied pressure. Moreover, at fixed pressure, while the rate constants of the reactions $4H_2$+Ti-CNC are smaller than those of $4H_2$+Ti-CNCS, the life times of the reactions $4H_2$+Ti-CNC are greater than those of $4H_2$+Ti-CNCS counterparts.

Conclusions

In the present study, the hydrogen storage capabilities of Ti functionalized CNC and CNCS are investigated by using density functional theory calculations, taking into account the long-range corrected hybrid density functional with damped atom-atom dispersion corrections . Based on the present results, gravimetric capacity, physisorption and thermodynamic properties of hydrogen storage reactions meet the ultimate targets of DOE for practical applications on the outer surface of Ti-CNC as well as on both sides of Ti-CNCS at 233.15 K. Favorable kinetics are also noticed at the temperatures targeted by DOE regardless of the applied pressure. The examined systems may therefore provide guidelines for the development of solid state hydrogen storage materials.

References

[1] N. S. Venkataramanan, H. Mizuseki and Y. Kawazoe, NANO: Brief reports and reviews., 2009, 4, 253-263.

[2] J. Yang, A. Sudik, C. Wolverton and D. J. Siegel, Chem. Soc. Rev., 2010, 39, 656-675.

[3] H. Tanaka, H. Kanoh, M. El-Merraoui, W. A. Steele, M. Yudasaka and S. Ijiima, J. Chem. Phys. B., 2004, 108, 17457–17465 .

[4] Y. Yurum, A. Taralp and T. N. Veziroglu, I. J. Hydrogen. energy ., 2009, 34, 3784-3798.

[5] R. Strobel, J. Garche, P. T. Moseley, L. Jörissen and G. Wolf, J. Power. Source., 2006, 159, 781-801

[6] E. Durgun, S. Ciraci, W. Zhou, and T. Yildirim, Phys. Rev. Lett., 2006., 97, 226102-4.

[7] Z. M. Ao and Q. Jiang, The open nanoscience journal., 2009, 3, 34-55.

[8] J.-D. Chai and M. Head-Gordon, Phys. Chem. Chem. Phys., 2008, 10, 6615-20.

[9] M.J. Frisch, G.W. Trucks, H.B. Schlegel, G.E. Scuseria, M.A. Robb, J.R.Cheeseman, Gaussian, Inc., Wallingford CT, 2010.

[10] N. M. O'Boyle, A. L. Tenderholt and K. M. Langner, J. Comput. Chem., 2008, 29, 839-845.

[11] S. Berber and D. Tomanck, Phys. Rev. B., 2009, 80, 075427-5

[12] V. Tozzini and V. Pellegrini, J. Phys. Chem. C., 2011, 115, 25523-25528.

[13] T. Yildirim and S. Ciraci, Phys. Rev. Lett., 2005, 94, 175501-4.

[14] J. J. Reilly and R. H. Wiswall, Inorg. Chem., 1968, 7, 2254-56.

[15] H. McKay, D.J.Wales, S.J.Verges and P.L.deAndres, Phys. Rev. B., 2010, 81, 075425-6.

Table 1: Structural and energetic properties of the optimized systems. Average adsorption energies per H_2 ($\Delta E_{ads.}$) correctd for dispersion forces are given in eV, distances (d) are in Å, and natural bond order charges (Q) in a.u.

	ΔE_{ads}	$d_{Ti\text{-}CNC}$	$d_{Ti\text{-}H}$	$d_{H\text{-}H}$	Q_{Ti}	Q_C	$Q_{H\text{-}H}$
$4H_2$-Ti-CNC	-0.54	2.09 3.67	1.96 1.97	0.78 0.79 0.79 0.79	0.47	-0.16 -0.15	0.0260, 0.0423 0.0289, 0.0670 0.0371, 0.0491 0.0362, 0.0475
$4H_2$-Ti-CNCS	-0.39	1.95 2.54	1.94 1.95	0.78 0.78 0.79 0.79	0.50	-0.05 -0.15	0.0429, 0.0557 0.0450, 0.0662 0.0436, 0.0546 0.0446, 0.0672

Table 2: The (min./max.) temperatures (T), (min./max.) pressures (P), free energy change (ΔG), enthalpy change (ΔH), thermal energy(E_t), heat capacity at constant volume (C_v), entropy change (ΔS), entropy change terms, and surface coverage (θ) of the hydrogen storage reactions

$4H_2 + \text{Ti-CNC} \rightarrow 4H_2\text{-Ti-CNC}$

T(^{o}C/K)	P(MPa/atm.)	ΔG (kcal/mol)	ΔH (kJ/mol H_2)	(E_t) kcal/mol	C_V Cal/K.mol	ΔS Cal/K.mol	ΔS_{trans} Cal/K.mol	ΔS_{elec} Cal/K.mol	ΔS_{vib} Cal/K.mol	ΔS_{rot} Cal/K.mol	θ
105/378.15	1.2/11.8430792	-4.96	-40.22	338.235	226.338	-88.529	-97.369	0.0	22.866	-14.025	0.999
105/378.15	0.3/2.9607698	-0.79	-40.22	338.235	226.338	-99.549	-108.393	0.0	22.865	-14.025	0.895
-40/233.15	1.2/11.8430792	-17.57	-38.97	311.495	138.442	-84.376	-87.76	0.0	13.562	-10.181	1.00
-40/233.15	0.3/2.9607698	-14.99	-38.97	311.495	138.442	-95.398	-98.781	0.0	13.564	-10.181	1.00

$4H_2 + \text{Ti-CNCS} \rightarrow 4H_2\text{-Ti-CNCS}$

T(^{o}C/K)	P(MPa/atm.)	ΔG (kcal/mol)	ΔH (kJ/mol H_2)	(E_t) kcal/mol	C_V Cal/K.mol	ΔS Cal/K.mol	ΔS_{trans} Cal/K.mol	ΔS_{elec} Cal/K.mol	ΔS_{vib} Cal/K.mol	ΔS_{rot} Cal/K.mol	θ
105/378.15	1.2/11.8430792	-5.04	-28.39	330.713	238.283	-85.068	-97.369	0.0	26.284	-13.983	0.999
105/378.15	0.3/2.9607698	-9.21	-28.39	330.713	238.283	-96.087	-108.393	0.0	26.285	-13.983	0.999
-40/233.15	1.2/11.8430792	-7.11	-27.37	302.053	135.801	-81.684	-87.76	0.0	16.212	-10.14	0.999
-40/233.15	0.3/2.9607698	-4.54	-27.37	302.053	152.524	-92.704	-98.781	0.0	16.216	-10.14	0.999

Table 3: Infrared (IR) spectra of H_2: (H(71)-H(72), H(73)-H(4),H(75)-H(76), H(77)-H(78) in $4H_2$-Ti-CNC and $4H_2$-Ti-CNCS complexes in the gas phase calculated at the wb97xd/6-31g(d,p) level of theory.

	Frequency (Cm^{-1})	Force constant (m Dyne/Å)	Dipole strength (10^{-40} esu^2 Cm^2)
$4H_2$-Ti-CNC H(71)-H(72)	3548	7.4795	496
H(73)-H(74)	3578	7.6085	423
H(75)-H(76)	3637	7.8560	269
H(77)-H(78)	3676	8.0283	843
$4H_2$-Ti-CNCS H(71)-H(72)	3629	7.8234	169
H(73)-H(74)	3658	7.9491	232
H(75)-H(76)	3675	8.0233	922
H(77)-H(78)	3749	8.3479	63

Table 4: The temperatures (T), life times (τ) and rate constants (k) of the reactions $4H_2$+Ti-CNC and $4H_2$+Ti-CNCS. As we increase the temperature, the life time drops and rate constant increases.

$4H_2$+Ti-CNC

T(K)	τ (s)	k (s^{-1})
378.15	0.130×10^{-9}	$0.760\times10^{+8}$
233.15	0.198×10^{-6}	$0.505\times10^{+5}$

$4H_2$+Ti-CNCS

T(K)	τ (s)	k (s^{-1})
378.15	3.07×10^{-10}	$3.26\times10^{+9}$
233.15	4.99×10^{-8}	$2.01\times10^{+7}$

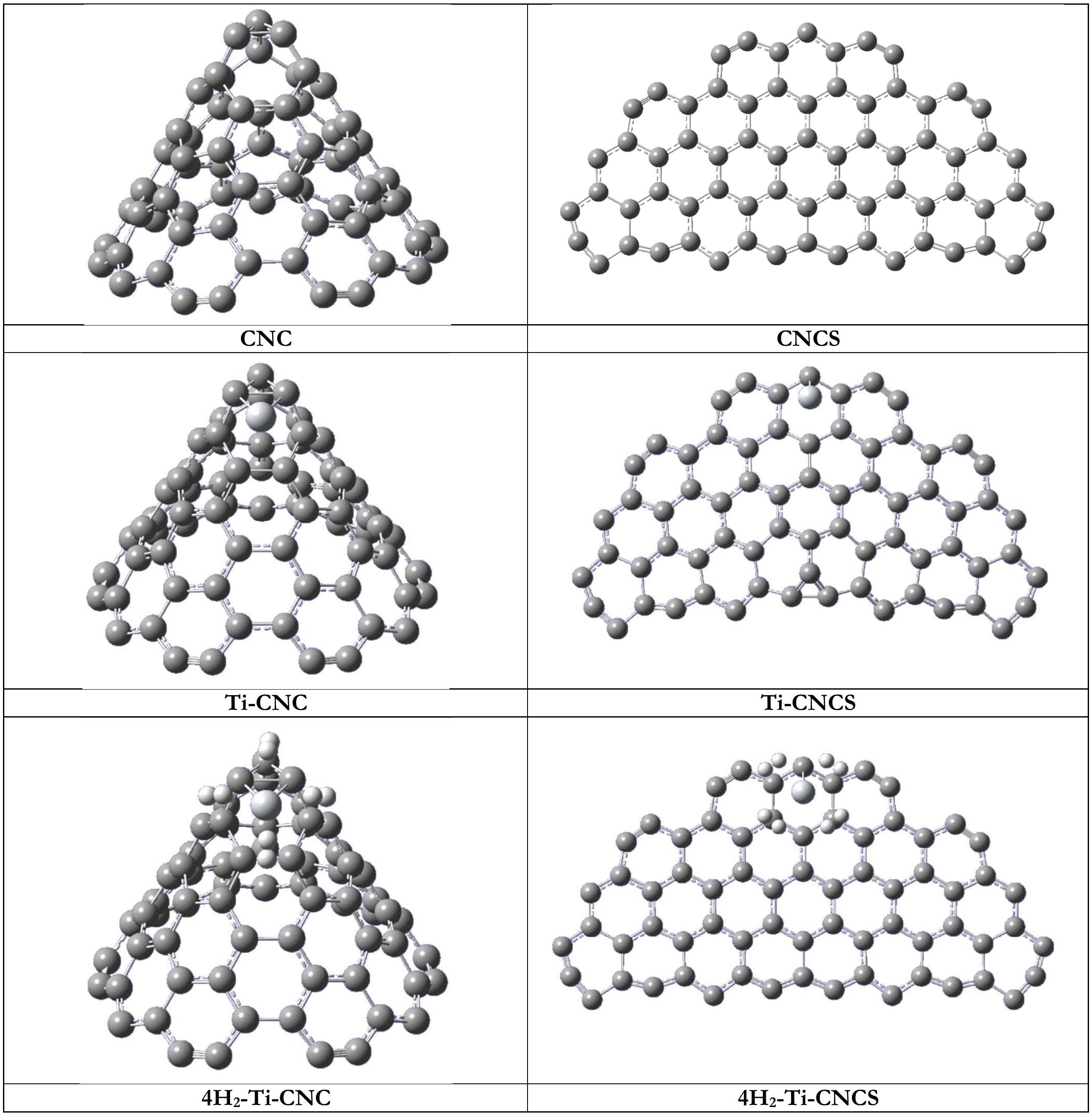

CNC CNCS

Ti-CNC Ti-CNCS

$4H_2$-Ti-CNC $4H_2$-Ti-CNCS

Fig.1: The optimal geometries of CNC, CNCS, Ti-CNC, Ti-CNCS, $4H_2$-Ti-CNC, and $4H_2$-Ti-CNCS at the wb97xd/6-31g(d,p) level of theory.

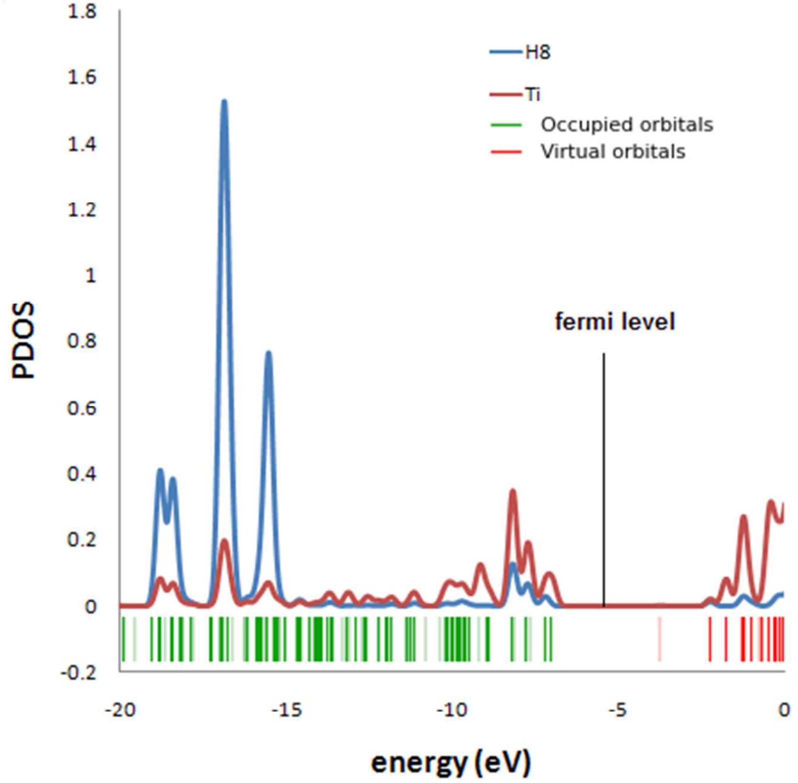

4H2-Ti-CNC

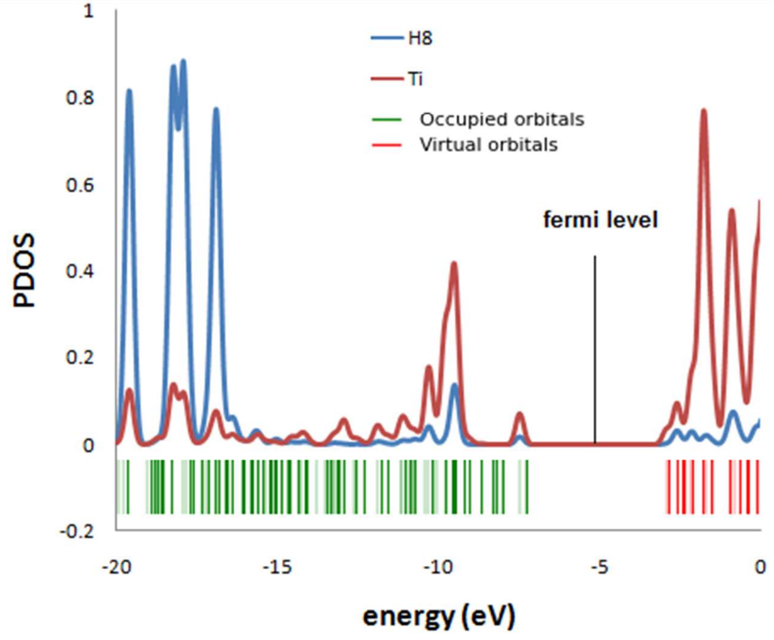

4H2-Ti-CNCS

Fig.2: Projected densities of states (PDOS) of $4H_2$-Ti-CNC and $4H_2$-Ti-CNCS.